Draft version March 3, 2023
Typeset using LaTeX **preprint2** style in AASTeX63

TESS observations of the Pleiades cluster: a nursery for δ Scuti stars

Timothy R. Bedding,[1] Simon J. Murphy,[2] Courtney Crawford,[1] Daniel R. Hey,[3] Daniel Huber,[3] Hans Kjeldsen,[4] Yaguang Li (李亚光) ,[1] Andrew W. Mann,[5] Guillermo Torres,[6] Timothy R. White,[1] and George Zhou[2]

[1]*Sydney Institute for Astronomy, School of Physics, University of Sydney NSW 2006, Australia*
[2]*Centre for Astrophysics, University of Southern Queensland, Toowoomba, QLD 4350, Australia*
[3]*Institute for Astronomy, University of Hawai'i, Honolulu, HI 96822, USA*
[4]*Stellar Astrophysics Centre, Department of Phsyics and Astronomy, Aarhus University, 8000 Aarhus C, Denmark*
[5]*Department of Physics and Astronomy, University of North Carolina at Chapel Hill, Chapel Hill, NC, USA*
[6]*Center for Astrophysics | Harvard & Smithsonian, 60 Garden St., Cambridge, MA 02138, USA*

ABSTRACT

We studied 89 A- and F-type members of the Pleiades open cluster, including five escaped members. We measured projected rotational velocities ($v \sin i$) for 49 stars and confirmed that stellar rotation causes a broadening of the main sequence in the color-magnitude diagram. Using time-series photometry from NASA's *TESS* Mission (plus one star observed by *Kepler*/K2), we detected δ Scuti pulsations in 36 stars. The fraction of Pleiades stars in the middle of the instability strip that pulsate is unusually high (over 80%), and their range of effective temperatures agrees well with theoretical models. On the other hand, the characteristics of the pulsation spectra are varied and do not correlate with stellar temperature, calling into question the existence of a useful $\nu_{\rm max}$ relation for δ Scutis, at least for young main-sequence stars. By including δ Scuti stars observed in the *Kepler* field, we show that the instability strip is shifted to the red with increasing distance by interstellar reddening. Overall, this work demonstrates the power of combining observations with Gaia and *TESS* for studying pulsating stars in open clusters.

Keywords: Asteroseismology

1. INTRODUCTION

Explaining the details of excitation and mode selection in δ Scuti stars is one of the major unsolved challenges in stellar pulsations (see reviews by Goupil et al. 2005; Handler 2009; Lenz 2011; Guzik 2021; Kurtz 2022). Why do only a subset of stars in the instability strip show δ Scuti pulsations? And how can two stars occupy essentially the same position in the H–R diagram, but only one shows pulsations?

One obvious explanation is that some stars have pulsations too weak to be detected. However, CoRoT and *Kepler* pushed the detection threshold down to extremely low levels (Balona et al. 2015; Michel et al. 2017; Bowman & Kurtz 2018; Guzik 2021), and it is still the case that only about half the stars in the central part of

Corresponding author: Timothy R. Bedding
tim.bedding@sydney.edu.au

the instability strip are pulsating (Murphy et al. 2019).

Another possible factor is chemical composition. Stars with different metallicities can pass through a given location in the H–R diagram at different ages, and with different opacities in the driving zone. This will affect pulsations driven by the κ (opacity) mechanism (Guzik et al. 2018), and even more so for chemically peculiar stars (Murphy et al. 2015; Guzik et al. 2021), so it is likely that chemical composition is part of the explanation. But even in open clusters, which are assumed to have a uniform metallicity (De Silva et al. 2006; Sestito et al. 2007; Bovy 2016), the pulsator fraction is much less than one. In the Pleiades, for example, Breger (1972) found four δ Scuti stars and three decades later, that number still only stood at six (Koen et al. 1999; Li et al. 2002; Fox Machado et al. 2006). *Kepler*/K2 observed five of these in short-cadence (1-min) mode (Murphy et al. 2022), and the long-cadence (30-min) data hinted at more variables (Rebull et al. 2016).

NASA's *TESS* Mission (Ricker et al. 2015) is producing high-precision, rapid-cadence light curves over most of the sky, opening up new possibilities for studying large samples of δ Scuti stars (e.g., Antoci et al. 2019; Balona & Ozuyar 2020; Barceló Forteza et al. 2020; Bedding et al. 2020; Murphy et al. 2020). In this *Letter*, we use data from Gaia and *TESS* to perform the most detailed search to date for δ Scuti pulsators in the Pleiades open cluster (Messier 45).

2. SAMPLE SELECTION AND GAIA PHOTOMETRY

We selected an initial list of likely Pleiades members using Gaia DR2 astrometry and the BANYAN-Σ code (Gagné et al. 2018). We used the default Pleiades parameters and did not include any radial velocity information (to avoid biasing against binaries). We selected all stars with BANYAN membership probabilities above 90% and Gaia colors $0.0 < G_{BP} - G_{RP} < 0.7$, which corresponds approximately to spectral types in the range A0 V to F8 V. This gave a list of 83 stars. We note that our membership selection was not altered by updating to Gaia DR3.

We also included five stars listed by Heyl et al. (2022) as escaped Pleiades members (HD 17962, HD 20655, HD 21062, HD 23323 and HD 34027). These stars are too distant from the Pleiades core to have been included in our BANYAN-Σ selection. We note that a cross-check of the G and early K dwarfs in the Heyl et al. (2022) sample with *TESS* indicated most of the suggested escapees have < 10 day rotation periods, which is consistent with expectations for Pleiades membership (Curtis et al. 2019).

Our final sample of 89 stars is listed in Table 1. V1229 Tau (HD 23642) is a well-studied eclipsing and spectroscopic binary that consists of two A-type stars with an orbital period of 2.4611 d (see Groenewegen et al. 2007, and references therein). Both components are A-type stars, so we have listed them separately in the table (see Sec. 4.1 for details).

Ten stars in Table 1 are named variables (column 1). These include the six δ Scuti stars previously known from ground-based observations (V534 Tau, V624 Tau, V647 Tau, V650 Tau, V1187 Tau and V1228 Tau; Breger 1972; Koen et al. 1999; Li et al. 2002), together with two γ Doradus stars (V1210 Tau and V1225 Tau; Martín & Rodríguez 2000) and both members of the eclipsing binary V1229 Tau (HD 23642).

The photometry in Table 1 (columns 4–6) is based on magnitudes and parallaxes from Gaia DR3 (Gaia Collaboration 2021; Lindegren et al. 2021; Riello et al. 2021). In Fig. 1 we show the color-magnitude diagram (CMD) of the sample. No correction for extinction or reddening was made. We have included a PARSEC isochrone (Marigo et al. 2017), with a metallic-

ity of $Z = 0.017$ and an age of 110 Myr, which are appropriate for the Pleiades (Gaia Collaboration et al. 2018). We shifted the isochrone to account for extinction and reddening, using values of $A_G = 0.11$ and $E(G_{BP} - G_{RP}) = 0.055$ (Andrae et al. 2018).

Some of the spread in the cluster main sequence is from binarity. The red circles in Fig 1a mark known spectroscopic binaries from the list compiled by Torres et al. (2021), and some of these clearly lie above the cluster sequence. Figure1a also shows several stars above the main sequence with values of Gaia RUWE (renormalised unit weight error) significantly greater than 1.0, indicating they are likely to be binaries (Evans 2018; Belokurov et al. 2020). Note that stars with high RUWE values can still provide useful parallaxes, although generally with larger uncertainties (e.g., Lindegren et al. 2021; El-Badry et al. 2021; Maíz Apellániz et al. 2021). As a check, we examined the `fidelity_v2` diagnostic calculated by Rybizki et al. (2022) and found it to have a value of 1.0 for all stars in our sample, indicating the astrometric solutions are reliable.

We conclude that stars well above the cluster sequence have high RUWE, are spectroscopic binaries, or both. The remaining spread in the observed sequence can be attributed to the presence of rapid rotators, as discussed in the next section.

3. PROJECTED ROTATIONAL VELOCITIES

We have measured $v \sin i$ for 49 stars in our sample using spectra collected by the Center for Astrophysics (CfA) survey (Torres 2020; Torres et al. 2021). These were gathered with the Tillinghast Reflector Échelle Spectrograph (TRES), a high-resolution ($R = 44,000$) fiber-fed échelle mounted on the 1.5m reflector at the Fred Lawrence Whipple Observatory, Arizona. Following Zhou et al. (2018), we extracted line profiles from each spectrum via a least-squares deconvolution (Donati et al. 1997) against a synthetic non-rotating ATLAS9 template (Castelli & Kurucz 2003). The broadening profile was then modeled as a combination of kernels describing the effects of rotational, macroturbulent, and instrumental broadening (Gray 2005). The resulting $v \sin i$ values are listed in column 8 of Table 1 and are indicated as source 1 in column 9. For an additional 10 stars, we used $v \sin i$ measurements from Gaia RVS spectra (Creevey et al. 2022), which are indicated as source 2 in the table. By way of validation, we note there is good consistency for 15 stars with $v \sin i$ measurements from both sources. We also note that the distribution of our $v \sin i$ measurements is similar to that of A-type stars in general (e.g., Royer et al. 2007; Zorec & Royer 2012), so that we can consider the Pleiades to be representative of the broader population.

The color-magnitude diagram in Figure 1b is color-coded by $v \sin i$. It is well-known that rotation causes stars to move in the CMD (Pérez Hernández et al. 1999; Fox Machado et al. 2006; Espinosa Lara & Rieutord 2011; Lipatov & Brandt 2020; Wang et al. 2022; Malofeeva et al. 2023). This is at least partly responsible for the extended main-sequence turn-offs seen in the CMDs of young and intermediate-age clusters (Bastian & de Mink 2009; Yang et al. 2013; Brandt & Huang 2015; Goudfrooij et al. 2017; Gossage et al. 2019; Sun et al. 2019; de Juan Ovelar et al. 2020; Kamann et al. 2020; Chen et al. 2022a; He et al. 2022). Rotation does not only affect the turn-off, but also broadens the main sequence itself, and we are seeing good evidence for this in the Pleiades in Fig. 1b.

4. *TESS* OBSERVATIONS AND ANALYSIS

Observations with *TESS* are made in 27-d sectors (Ricker et al. 2015). The Pleiades were observed in the fourth year of the mission, in Sectors 42–44 (2021 August 20 to November 6). Most Pleiades stars have *TESS* data in all

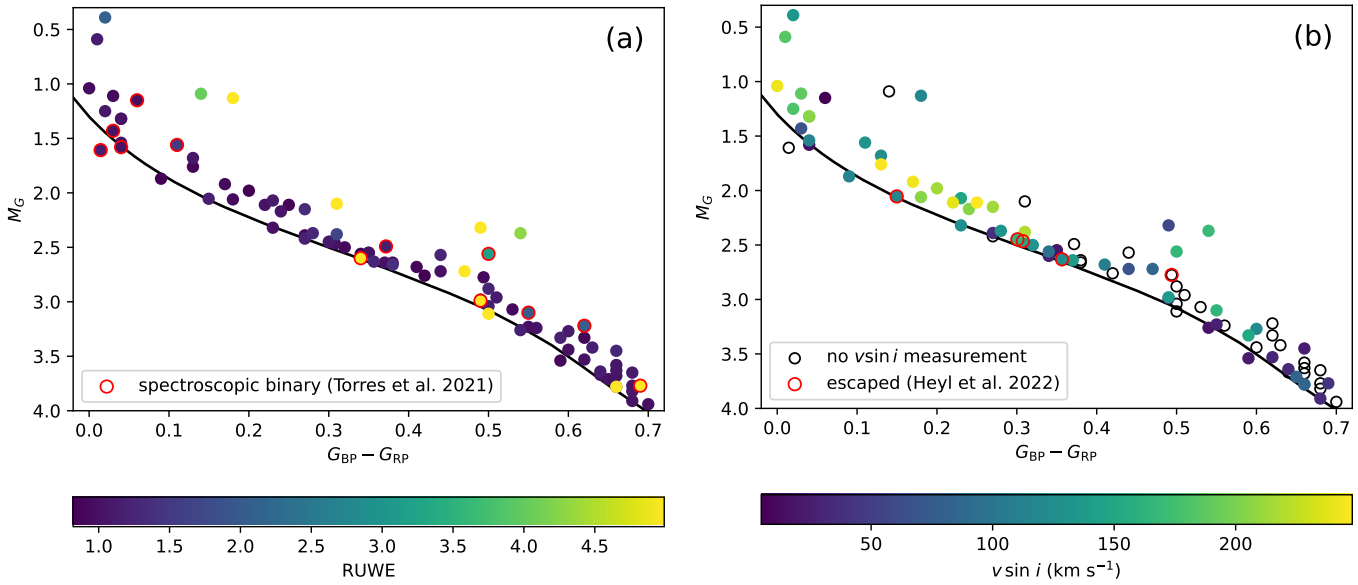

Figure 1. Color-magnitude diagram of 89 A and F stars in the Pleiades, based on photometry and parallaxes from Gaia DR3. Photometry has not been corrected for extinction and reddening. (a) Stars are color-coded by RUWE (clipped at RUWE = 5, although some stars have greater values) and red circles indicate spectroscopic binaries (Torres et al. 2021); (b) Stars are color-coded by $v \sin i$ (see Table 1) and red circles indicate five stars listed as escaped members by Heyl et al. (2022). The black line in both panels is a PARSEC isoschrone, corrected for extinction and reddening (see text).

three sectors and a few were also observed in Sectors 18 or 19. All the stars in our sample except two have *TESS* observations with 120-s cadence, and we used the `lightkurve` package (Lightkurve Collaboration et al. 2018) to download the PDCSAP[1] light curves that were provided by the SPOC (Science Processing Operations Center). The first exception was HD 23479. For this star we extracted a light curve from the *TESS* full-frame images (10-min cadence), which showed no evidence for δ Scuti pulsations.[2] The second exception was HD 23028, which fell just off the edge of the detector and is the only star in our sample with no *TESS* observations. For this star, *Kepler*/K2 long-cadence (30-min) observations show pulsations and we have included it as a δ Scuti star in the table and figures (apart from Fig. 2).

In total, we detected δ Scuti pulsations in 36 of the stars in our sample, as flagged in Table 1 (column 10). These include the six previously known from ground-based observations (V534 Tau, V624 Tau, V647 Tau, V650 Tau, V1187 Tau and V1228 Tau), plus 30 additional detections. For all detections, the amplitude spectrum showed several clear peaks at least 10 times the mean noise level (and often much higher), while the non-detections showed no significant peaks above about 4 times the noise. The last two columns of Table 1 show the frequency and amplitude of the strongest mode in each δ Scuti star (measured in the range 10 to 80 d^{-1}).

The amplitude spectra for the 35 δ Scuti stars observed by *TESS* are shown in Fig. 2, ordered according to Gaia $G_{BP} - G_{RP}$. The detections include four of the five escaped members (Heyl et al. 2022), and the similarity of those os-

[1] Pre-search Data Conditioning Simple Aperture Photometry

[2] The light curve for HD 23479 was contaminated by oscillations from HD 23463 (separation 39 arcsec), which is a red giant whose parallax and proper motion show it to be currently passing through the Pleiades cluster.

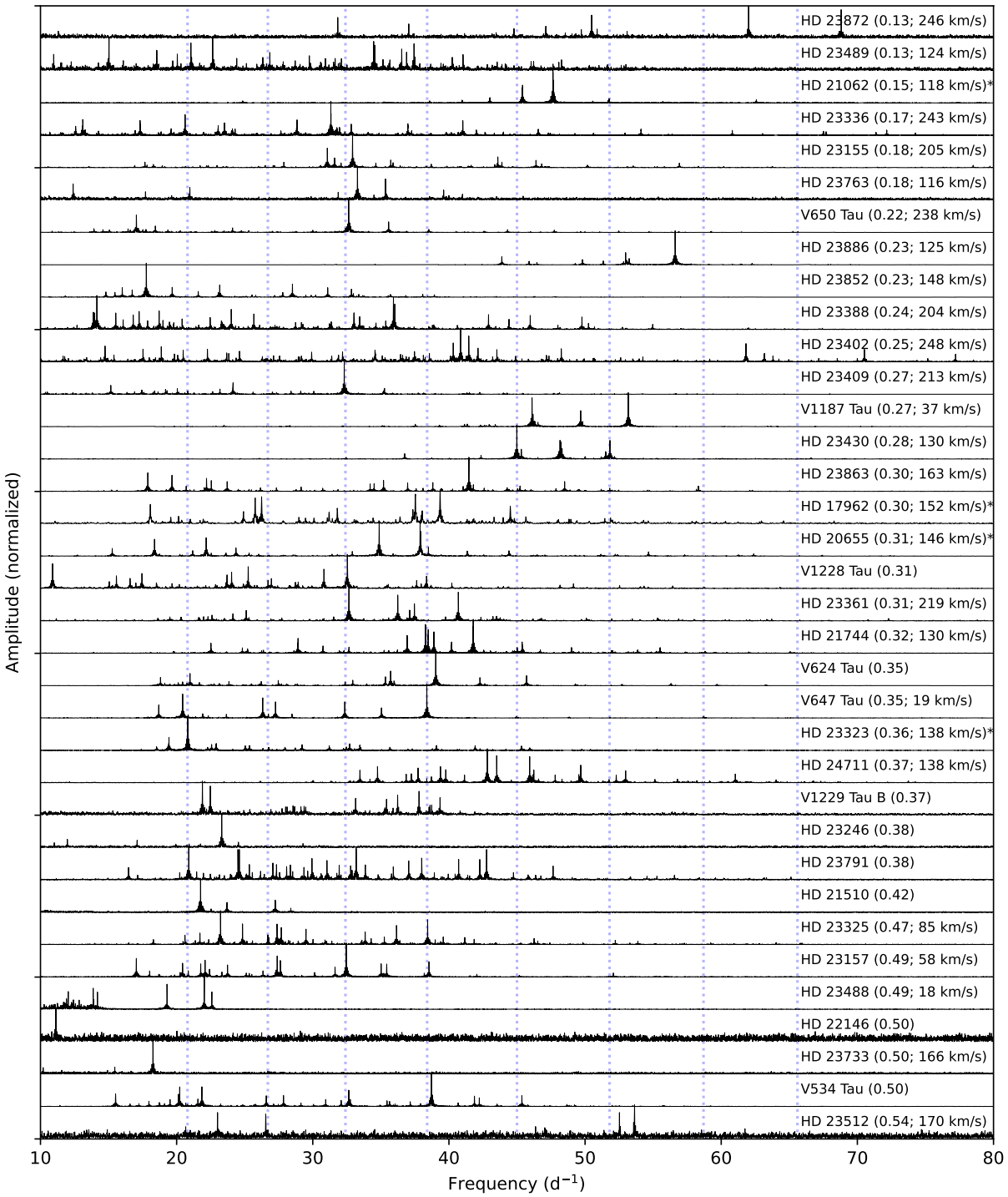

Figure 2. Pulsation spectra of 35 δ Scuti stars in the Pleiades observed with *TESS*. Stars are ordered according to the Gaia $G_{BP} - G_{RP}$ color index, whose values are given in parentheses, together with $v \sin i$ (if available). Asterisks indicate four stars listed by Heyl et al. (2022) as escaped members. To help guide the eye, the blue dotted lines show approximate frequencies of the first 8 radial modes (see Sec. 6). These are based on the observed frequencies in the star V647 Tau, which has a particularly regular spectrum (Murphy et al. 2022, Table 4).

cillation spectra to confirmed members of the Pleiades lends support to their status as escaped members.

4.1. *V1229 Tau (HD 23642)*

V1229 Tau is a well-studied eclipsing and spectroscopic binary, with a period of 2.4611 d (see Groenewegen et al. 2007, and references therein). Both components are A-type stars, and so we have treated them separately.

The Gaia photometry ($G = 6.82$ and $G_{BP} - G_{RP} = 0.10$) measures the combined light of the system. In order to plot both components separately, we have estimated values in the table using the published effective temperatures (9750 ± 250 K and 7600 ± 400 K; Southworth et al. 2005) and a luminosity ratio of 0.355 ± 0.035 (David et al. 2016). The photometry given in columns 4–6 of Table 1 are estimates if the two components were measured separately, also taking into account the reddening and extinction of the cluster. In Fig. 3a, the black circles show (from left to right) the A component, the combined system, and the B component.

In addition to the eclipses, the *TESS* light curve shows high-frequency δ Scuti pulsations. The amplitude spectrum in Fig. 2 was made after fitting and subtracting an eclipse model. Given the colors of the components (see Fig. 3a), it is reasonable to conclude that the pulsations occur in the B component. To verify this, we examined the scatter in the time series after fitting and removing the five highest peaks in the amplitude spectrum. We found the scatter to be reduced everywhere in this prewhitened light curve, but the reduction was less during secondary eclipses because the five-peak fit is a poorer fit when part of the pulsating star is being eclipsed (note that the inclination of the system is about 78° and the eclipses are not total; David et al. 2016). We can therefore confirm that it is the secondary component (V1229 Tau B) that is undergoing pulsations.

Chen et al. (2022b) noted pulsations in V1229 Tau (which they referred to as TIC 125754991) and suggested that it is hotter than typical δ Scuti stars, because they assumed the primary is the pulsator. Once we accept that the secondary is the pulsating component, this star becomes typical. A more detailed study of the pulsations of V1229 Tau (HD 23642) using the *TESS* light curve has been made by Southworth et al. (in prep.).

5. THE δ SCUTI INSTABILITY STRIP

Figure 3 shows the δ Scuti detections as a function of Gaia $G_{BP} - G_{RP}$ color index (without correcting for the reddening of the Pleiades, which is about 0.055; Andrae et al. 2018). We see in the CMD (Fig. 3a) and the accompanying histogram (Fig. 3b) that the pulsators lie within a strip that spans from about 0.10 to 0.55 in $G_{BP} - G_{RP}$. In this color range, the fraction of stars that pulsate is 36/50 ($72 \pm 6\%$), and in the middle of the instability strip (0.20–0.40) it is 21/25 ($84 \pm 7\%$). This pulsator fraction is significantly higher than the 50–60% found in the *Kepler* δ Scuti sample by Murphy et al. (2019).

Although the Pleiades cluster is unusually rich in δ Scutis (with peak amplitudes in the range 50–3000 ppm, depending on the star), there are still several stars within the instability strip that are not pulsating (down to a sensitivity limit of 10–20 ppm). One possible explanation is chemical peculiarity, which typically occurs in slow rotators because helium sinks out of the He II driving zone (Baglin et al. 1973; Deal et al. 2020). Slow rotation can be caused by tidal interactions with a binary companion (e.g., Fuller et al. 2017, and references therein), which is thought to be responsible for the Am stars ('m' for 'metallic-lined'; e.g., Abt 1967; North et al. 1998; Debernardi et al. 2000; Stateva et al. 2012).

Eight stars in our sample were listed by Renson & Manfroid (2009) as being Am stars (see column 11 in Table 1). One of these is the eclips-

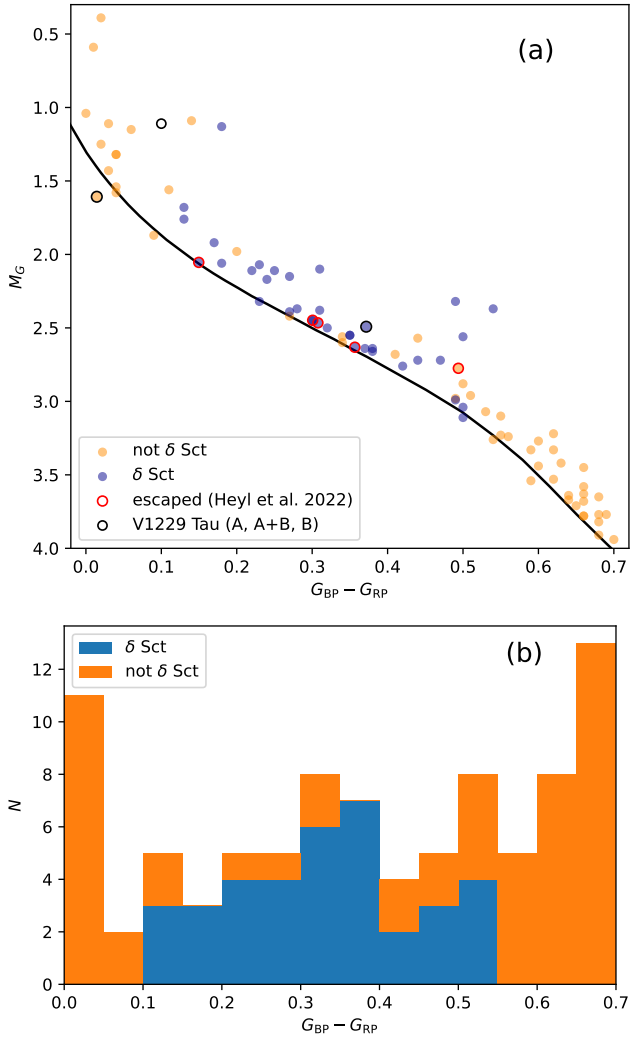

Figure 3. Sample of 89 A and F stars in the Pleiades, of which 36 show δ Scuti pulsations (orange) and 53 do not (blue). (a) Color-magnitude diagram, where red circles are the five escaped members (Heyl et al. 2022). For the eclipsing binary V1229 Tau (HD 23642), black circles show (from left to right) the A component (not pulsating), the combined system, and the B component (pulsating; see text). The black line is a PARSEC isoschrone (corrected for extinction and reddening; see text). (b) Histogram as a function of Gaia color.

ing binary V1229 Tau, for which Abt & Levato (1978) give the spectral type as A0 Vp(Si) + Am, indicating that the B component is an Am star. Overall, seven of the Am stars in our sample have colours that place them within the δ Scuti instability strip, and five of these are

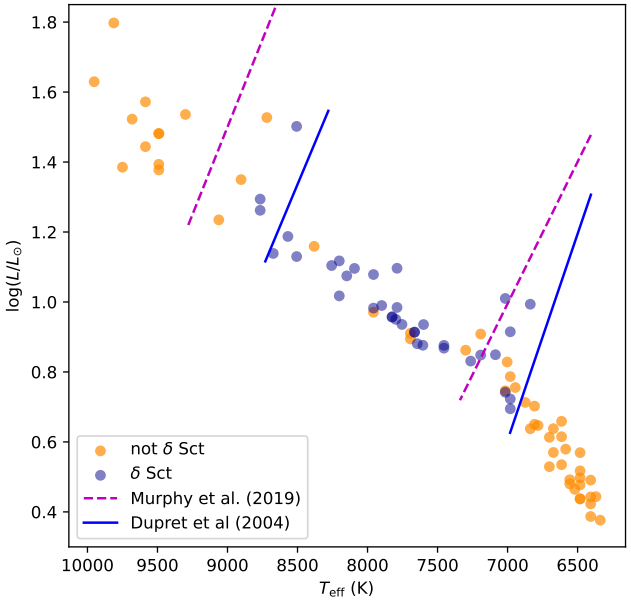

Figure 4. H–R diagram of the Pleiades, corrected for extinction and reddening, showing the location of the δ Scuti pulsators. Sloping lines indicate both the theoretical instability strip (solid blue lines; Dupret et al. 2005) and the observed strip from *Kepler* (dashed purple lines show the region in which at least 20% of *Kepler* stars pulsate; Murphy et al. 2019).

pulsating. The conclusion is that chemical peculiarity can only account for two of the non-pulsators in the Pleiades.

Figure 4 shows our sample in an H–R diagram. To construct this, we first corrected the observed Gaia photometry for extinction and reddening using the values given above. We estimated effective temperatures from the de-reddened $G_{BP} - G_{RP}$ colors using an updated version of Table 5 of Pecaut & Mamajek (2013)[3]. We estimated approximate stellar luminosities from G magnitudes and Gaia DR3 parallaxes, using V bolometric corrections and $G - V$ colours from the same source.

[3] http://www.pas.rochester.edu/~emamajek/EEM_dwarf_UBVIJHK_colors_Teff.txt

The solid blue lines in Fig. 4 show the theoretical instability strip calculated by Dupret et al. (2005), which used a typical solar composition ($X = 0.7$, $Z = 0.02$), a convective core overshooting parameter of $\alpha_{ov} = 0.2$, and a solar-calibrated value for the mixing length parameter ($\alpha_{MLT} = 1.8$). With the caveat that α_{MLT} could have a different value for the Pleiades, we conclude that the observed δ Scuti strip for our sample is quite well matched to the theoretical calculations.

The dashed purple lines in Fig. 4 mark the instability strip for δ Scuti stars observed with *Kepler* (Murphy et al. 2019). The offset with respect to the Pleiades might come from a combination of: (1) different $T_{\rm eff}$ scales being used; (2) having a homogeneous composition among Pleiades members, rather than the heterogeneous *Kepler* sample; (3) perhaps from having a slightly higher overall metallicity in the Pleiades; (4) from the Pleiades being young, as opposed to the *Kepler* sample where some stars that appeared near the ZAMS may be older stars of lower metallicity; and (5) the larger *Kepler* sample may give rise to more outliers at the hotter end of the distribution.

Figure 5 shows the effect of reddening on the δ Scuti instability strip by plotting the distance to each star versus its Gaia color index. The red points at the bottom show the Pleiades and the blue points show δ Scuti stars detected by *Kepler* (Murphy et al. 2019). As expected, the observed instability strip shifts to the red with increasing distance. Note that we have restricted the *Kepler* sample to stars more than 10 degrees from the Galactic plane, in order to see the dependence on distance more clearly. We see that the reddening in $G_{BP} - G_{RP}$ is approximately 0.15 magnitudes for every kpc in distance. We also show the sample of γ Doradus stars in the *Kepler* field studied by Li et al. (2020), again restricted to $b > 10°$ (orange points). Overall, Fig. 5 displays very nicely the effect of interstellar reddening on the pulsational instability strips. Note that we have not given a list of γ Doradus stars in the Pleiades, although many are certainly present, because having only a few *TESS* sectors often makes it difficult to distinguish unambiguously between gravity-mode pulsations and rotational modulation.

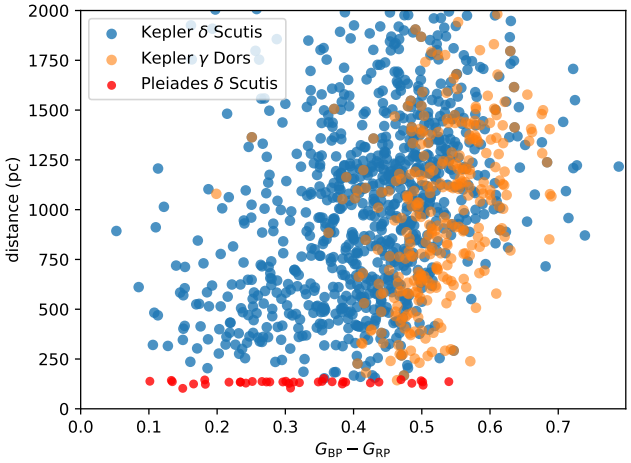

Figure 5. The effect of reddening on the pulsation instability strip. The *Kepler* samples of δ Scuti stars (from Murphy et al. 2019) and γ Doradus stars (Li et al. 2020) are restricted to Galactic latitude $b > 10°$.

6. IS THERE A $\nu_{\rm max}$ SCALING RELATION FOR δ SCUTI STARS?

The quantity $\nu_{\rm max}$ is defined for solar-like oscillations as the centroid of the power envelope (Kjeldsen & Bedding 1995). Solar-like oscillations are excited stochastically by near-surface convection, and the observed modes cover a broad range of frequencies centred at $\nu_{\rm max}$. It was suggested by Brown et al. (1991) that when scaling from the Sun to other stars, $\nu_{\rm max}$ should be a fixed fraction of the acoustic cutoff frequency. The latter is the frequency above which waves are no longer reflected at the surface, and is expected from simple arguments to scale as $g/\sqrt{T_{\rm eff}}$. That line of reasoning underlies the scaling relation

$$\nu_{\rm max} \propto g/\sqrt{T_{\rm eff}}, \qquad (1)$$

which is widely used in the study of solar-like oscillations, although its physical basis is not well understood (Belkacem et al. 2011; Kjeldsen & Bedding 2011; Chaplin & Miglio 2013; Hekker 2020).

There have been suggestions that $\nu_{\rm max}$ is a useful observable for δ Scuti stars, given that it shows a correlation with $T_{\rm eff}$ (Balona & Dziembowski 2011; Barceló Forteza et al. 2018; Bowman & Kurtz 2018; Barceló Forteza et al. 2020; Hasanzadeh et al. 2021). However, the oscillation spectra of δ Scuti stars in the Pleiades (see Fig. 2, which is ordered by color index) show the correlation to be weak or nonexistent for this sample of young main-sequence stars. In particular, we do not see a shift to higher radial orders with increasing $T_{\rm eff}$, as predicted by theoretical models. Different theoretical treatments give slightly different predictions, but they all agree that we expect the excitation of higher radial order modes in δ Scuti stars as we move to higher temperatures within the instability strip (Dziembowski 1997; Houdek et al. 1999; Pamyatnykh 2000; Dupret et al. 2005; Houdek & Dupret 2015; Xiong et al. 2016; Xiong 2021).

It is also worth noting that there is no unambiguous definition for $\nu_{\rm max}$ in δ Scuti stars. In a star with solar-like oscillations, the stochastic nature of the excitation and damping from convection leads to a power envelope of modes that is roughly Gaussian, with a well-defined maximum. In many δ Scuti stars, on the other hand, the distribution of amplitudes is much less ordered (see Fig. 2). Therefore, even defining what is meant by $\nu_{\rm max}$ in δ Scuti stars is not straightforward. One approach is to use the frequency of the strongest mode, f_1, which we have listed in Column 14 of Table 1. Given that many stars in Fig. 2 have several modes with similar amplitudes, this is clearly not an ideal metric. Not surprisingly, given the diversity in Fig. 2, we found that plots of f_1 versus various stellar parameters (such as $T_{\rm eff}$ and $v \sin i$) did not show no obvious correlations.

The variety of oscillation spectra in Fig. 2 is quite remarkable, although there is also similarity between some stars. To help guide the eye, the vertical dotted lines in the figure show the approximate locations of the first 8 radial modes. These are based on the observed frequencies in the star V647 Tau, which has a particularly regular spectrum (Murphy et al. 2022, Table 4).

It is well-established that oscillation frequencies (and therefore also the large separation, $\Delta\nu$) scale as the square root of stellar density (e.g., Aerts et al. 2010). Hence, we might expect $\Delta\nu$ to vary substantially among the Pleiades δ Scuti stars, given their range of masses. However, theoretical models of young main-sequence δ Scuti stars show that for fixed metallicity, $\Delta\nu$ is remarkably constant for a wide range of masses (see Fig.4a of Murphy et al. 2021 and Murphy et al., in prep.). This makes the vertical lines in Fig. 2 quite useful for comparing the oscillation spectra.

Some of the variations between stars could be attributed to differences in rotation, but it is difficult to see much in the way of systematic trends. Furthermore, the distribution of $v \sin i$ values in the Pleiades, as noted in Sec. 3, is similar to that of A-type stars in general. On balance, our results seem to raise more questions than they answer. On the one hand, the very high fraction of pulsators in the Pleiades means we are not left wondering why some pulsate and others do not. On the other hand, we cannot explain why stars with similar properties have such different pulsation spectra, although rotation presumably plays a role. An explanation for mode selection in δ Scuti stars remains as elusive as ever.

7. CONCLUSIONS

Using Gaia photometry and astrometry, we constructed a list of 89 probable members of

the Pleiades with spectral types A and F. We measured projected rotational velocities ($v \sin i$) for 49 stars and confirmed that stellar rotation is a significant cause of the broadening of the main sequence in the color-magnitude diagram (Fig. 1b). Using time-series photometry from NASA's *TESS* Mission (plus one star observed by *Kepler*/K2), we detected δ Scuti pulsations in 36 stars. Some stars suggested as being escaped members of the Pleiades by Heyl et al. (2022) have similar pulsation properties to confirmed members, which supports their identification as former members.

The fraction of Pleiades stars in the middle of the instability strip that pulsate is unusually high (over 80%), and their range of effective temperatures agrees well with theoretical models (Fig. 4). On the other hand, the characteristics of the pulsation spectra are very varied and do not correlate very strongly with stellar temperature (Fig. 2), calling into question the existence of a useful $\nu_{\rm max}$ relation for δ Scutis, at least for young stars. By including δ Scuti stars observed in the *Kepler* field (Fig. 5), we show that the instability strip is shifted to the red with increasing distance by interstellar reddening. In summary, this work demonstrates the power of combining observations with Gaia and *TESS* for studying pulsating stars in open clusters.

ACKNOWLEDGMENTS

We thank the *TESS* team for making this research possible. The *TESS* data used in this paper can be found in MAST: 10.17909/t9-nmc8-f686. We gratefully acknowledge support from the Australian Research Council through Discovery Project DP210103119, Future Fellowship FT210100485 and Laureate Fellowship FL220100117, and from the Danish National Research Foundation (Grant DNRF106) through its funding for the Stellar Astrophysics Centre (SAC). D.H. acknowledges support from the Alfred P. Sloan Foundation and the National Aeronautics and Space Administration (80NSSC21K0784). This research made use of Lightkurve, a Python package for *Kepler* and *TESS* data analysis (Lightkurve Collaboration et al. 2018). This work made use of several publicly available `python` packages: `astropy` (Astropy Collaboration 2013, 2018), `lightkurve` (Lightkurve Collaboration et al. 2018), `matplotlib` (Hunter 2007), `numpy` (Harris et al. 2020), and `scipy` (Virtanen et al. 2020).

This work has made use of data from the European Space Agency (ESA) mission Gaia (https://www.cosmos.esa.int/gaia), processed by the Gaia Data Processing and Analysis Consortium (DPAC, https://www.cosmos.esa.int/web/gaia/dpac/consortium). Funding for the DPAC has been provided by national institutions, in particular the institutions participating in the Gaia Multilateral Agreement. We thank the referee for useful comments on the paper.

Facility: TESS

Table 1. Sample of A and F stars in the Pleiades. Column 8: 1 indicates an escaped member (Heyl et al. 2022). Column 9: 1 indicates a spectroscopic binary (SB; Torres et al. 2021). Column 11: source for $v \sin i$ is 1 (this work) or 2 (Gaia DR3). Column 12: 1 indicates δ Scuti star. Column 13: 1 indicates Am star (Renson & Manfroid 2009). Columns 14 and 15: frequency and amplitude of the strongest δ Scuti mode. For V1229 Tau A & B, the magnitudes and colors (columns 5–7) are estimates (see Sec. 4.1).

Name	HD	HIP	TIC	G	M_G	$G_{BP} - G_{RP}$	Esc.	SB	$v \sin i$		δ Sct	Am	f_1	a_1
									km s^{-1}	src			d^{-1}	ppt
(1)	(2)	(3)	(4)	(5)	(6)	(7)	(8)	(9)	(10)	(11)	(12)	(13)	(14)	(15)
	22578	17000	113956708	6.70	1.04	0.00	0	0	242 ± 22	1	0	0		
24 Tau	23629		405484171	6.30	0.59	0.01	0	0	184 ± 15	1	0	0		
V1229 Tau A	23642	17704	125754991	7.32	1.61	0.01	0	1			0	0		
	23410	17572	67830155	6.90	1.25	0.02	0	0	180 ± 9	1	0	0		
	23950	17921	440695282	6.04	0.39	0.02	0	0	133 ± 7	1	0	0		
	24899	18559	149980785	7.20	1.43	0.03	0	1	67 ± 2	1	0	0		
	23568	17664	405484416	6.80	1.11	0.03	0	0	188 ± 5	2	0	0		
	22614	17034	427545204	7.10	1.54	0.04	0	0	114 ± 2	1	0	0		
	23631		440681316	7.29	1.58	0.04	0	1	13 ± 5	1	0	1		
	23632	17692	440681358	7.00	1.32	0.04	0	0	194 ± 3	2	0	0		
	23913	17892	440691760	7.00	1.32	0.04	0	0	205 ± 21	1	0	0		
	23964	17923	440695975	6.81	1.15	0.06	0	1	5 ± 1	1	0	0		
	23948		35159593	7.55	1.87	0.09	0	0	115 ± 1	2	0	0		
	22637	17043	113981021	7.27	1.56	0.11	0	1	131 ± 10	1	0	0		
	23872		346626001	7.53	1.76	0.13	0	0	246 ± 5	2	1	0	62.01	0.09
	23489		125736946	7.35	1.68	0.13	0	0	124 ± 2	1	1	0	22.64	0.08
	24076	17999	35205647	6.93	1.09	0.14	0	0			0	0		
	21062	15902	29058513	7.11	2.05	0.15	1	0	118 ± 1	2	1	0	47.64	1.05

Table 1 *continued*

Table 1 *(continued)*

Name	HD	HIP	TIC	G	M_G	$G_{BP} - G_{RP}$	Esc.	SB	$v \sin i$		δ Sct	Am	f_1	a_1
									km s^{-1}	src			d^{-1}	ppt
(1)	(2)	(3)	(4)	(5)	(6)	(7)	(8)	(9)	(10)	(11)	(12)	(13)	(14)	(15)
	23336	17547	385554826	7.40	1.92	0.17	0	0	243 ± 3	2	1	0	31.33	0.67
	23763	17791	35156298	6.94	1.13	0.18	0	0	116 ± 2	1	1	0	33.28	0.10
	23155	17403	405483425	7.51	2.06	0.18	0	0	205 ± 5	1	1	0	32.92	1.05
	24178		84336172	7.65	1.98	0.20	0	0	214 ± 13	1	0	0		
V650 Tau	23643		440681425	7.75	2.11	0.22	0	0	238 ± 7	1	1	0	32.64	2.97
	23886		346626099	7.96	2.32	0.23	0	0	125 ± 2	2	1	0	56.62	1.94
	23852		440691730	7.71	2.07	0.23	0	0	148 ± 4	1	1	0	17.77	1.59
	23388	17552	67828699	7.73	2.17	0.24	0	0	204 ± 7	1	1	0	14.14	0.51
	23402		67830321	7.80	2.11	0.25	0	0	248 ± 6	1	1	0	40.86	0.42
V1187 Tau	23194		405483707	8.04	2.39	0.27	0	0	37 ± 1	1	1	1	53.18	1.46
	23924		440695768	8.09	2.42	0.27	0	0			0	1		
	23409		385589694	7.83	2.15	0.27	0	0	213 ± 5	1	1	0	32.31	1.95
	23430	17583	385558439	8.02	2.37	0.28	0	0	130 ± 3	1	1	0	44.99	0.86
	23863		346626294	8.10	2.45	0.30	0	0	163 ± 6	1	1	0	41.47	1.28
	17962	13522	77568727	8.15	2.45	0.30	1	0	152 ± 2	2	1	0	39.35	0.57
	20655	15552	402366726	7.55	2.47	0.31	1	0	146 ± 2	2	1	0	34.88	1.38
	23361		385552144	8.02	2.38	0.31	0	0	219 ± 8	1	1	0	32.66	0.97
V1228 Tau	23628		125754823	7.63	2.10	0.31	0	0			1	0	32.54	0.74
	21744	16407	46476992	8.09	2.50	0.32	0	0	130 ± 3	1	1	0	41.78	0.81
	23664	17729	125754460	8.27	2.56	0.34	0	0	96 ± 2	1	0	0		
	23610	17694	440681752	8.12	2.60	0.34	0	1	26 ± 1	1	0	1		
V624 Tau	23156		405483817	8.20	2.55	0.35	0	0			1	0	39.03	1.67
V647 Tau	23607		405484188	8.24	2.55	0.35	0	0	19 ± 1	1	1	1	38.38	1.47

Table 1 *continued*

Table 1 *(continued)*

Name	HD	HIP	TIC	G	M_G	$G_{BP} - G_{RP}$	Esc.	SB	$v \sin i$		δ Sct	Am	f_1	a_1
									km s^{-1}	src			d^{-1}	ppt
(1)	(2)	(3)	(4)	(5)	(6)	(7)	(8)	(9)	(10)	(11)	(12)	(13)	(14)	(15)
	23323		385553714	8.55	2.63	0.36	1	0	123 ± 1	2	1	0	20.81	2.49
	24711	18431	14111056	8.30	2.64	0.37	0	0	138 ± 3	1	1	0	42.82	0.79
V1229 Tau B	23642	17704	125754991	8.20	2.49	0.37	0	1			1	1	21.89	0.15
	23246		348639016	8.12	2.64	0.38	0	0			1	0	23.31	0.19
	23791		440690782	8.34	2.66	0.38	0	0			1	1	20.89	0.38
V1210 Tau	23585		405484093	8.33	2.68	0.41	0	0	108 ± 3	1	0	0		
	21510	16217	405461432	8.33	2.76	0.42	0	0			1	0	21.75	0.45
	23479		385589599	8.23	2.57	0.44	0	0			0	0		
	23028	17325	114083179	8.36	2.72	0.44	0	0	68 ± 1	1	1	0		
	23325		385509282	8.55	2.72	0.47	0	0	85 ± 1	2	1	1	23.22	0.64
	23157	17401	67768222	7.86	2.32	0.49	0	0	58 ± 1	1	1	0	32.46	0.55
V1225 Tau	22702		427580304	8.75	2.98	0.49	0	0	137 ± 6	1	0	0		
	23488	17625	125736216	8.65	2.99	0.49	0	1	18 ± 1	1	1	0	22.04	0.88
	34027	24808	82969878	8.85	2.77	0.49	1	0			0	0		
	23375		385552372	8.55	2.88	0.50	0	0			0	0		
V534 Tau	23567		405484574	8.48	3.11	0.50	0	0			1	0	38.71	1.06
	23733		35155873	8.21	2.56	0.50	0	1	166 ± 25	1	1	0	18.26	0.16
	22146		26126738	8.79	3.04	0.50	0	0			1	0	11.13	0.05
	23290	17481	67788829	8.63	2.96	0.51	0	0			0	0		
	24132	18050	84331341	8.77	3.07	0.53	0	0			0	0		
	23326		67829720	8.89	3.26	0.54	0	0	19 ± 1	1	0	0		
	23512		61139371	8.04	2.37	0.54	0	0	170 ± 8	1	1	0	53.64	0.05
	23792		440690206	8.31	3.10	0.55	0	1	164 ± 11	1	0	0		

Table 1 *continued*

Table 1 *(continued)*

Name	HD	HIP	TIC	G	M_G	$G_{BP} - G_{RP}$	Esc.	SB	$v \sin i$		δ Sct	Am	f_1	a_1
									$\mathrm{km\,s^{-1}}$	src			$\mathrm{d^{-1}}$	ppt
(1)	(2)	(3)	(4)	(5)	(6)	(7)	(8)	(9)	(10)	(11)	(12)	(13)	(14)	(15)
	23289	17497	67787772	8.89	3.23	0.55	0	0	26 ± 1	1	0	0		
		16423	26078071	8.78	3.24	0.56	0	0			0	0		
	24655		14109779	8.98	3.54	0.59	0	0	22 ± 1	1	0	0		
	23912		440691379	9.03	3.33	0.59	0	0	151 ± 4	1	0	0		
	22887	17225	114060256	9.07	3.44	0.60	0	0			0	0		
	23133		114166637	8.89	3.27	0.60	0	0	122 ± 22	1	0	0		
	23351		385552643	8.90	3.22	0.62	0	1			0	0		
	23511		125736995	9.20	3.53	0.62	0	0	30 ± 1	1	0	0		
	24086		84331854	9.01	3.33	0.62	0	0			0	0		
	22977	17289	114084434	9.06	3.42	0.63	0	0			0	0		
	24302	18154	427735820	9.34	3.67	0.64	0	0			0	0		
	23513		61145701	9.30	3.64	0.64	0	0	32 ± 1	1	0	0		
	23584		405484278	9.38	3.71	0.65	0	0	82 ± 2	1	0	0		
	23312	17511	67788288	9.36	3.63	0.66	0	0			0	0		
		17125	353928999	9.50	3.78	0.66	0	0	85 ± 2	1	0	0		
	23514		61145611	9.31	3.58	0.66	0	0			0	0		
		18544	14177821	9.29	3.78	0.66	0	0	72 ± 2	1	0	0		
	23732		35155396	9.12	3.45	0.66	0	0	23 ± 1	1	0	0		
	23061		258067594	9.37	3.68	0.66	0	0			0	0		
SAO 93581			67789284	9.30	3.65	0.68	0	0			0	0		
	23975		35204900	9.52	3.82	0.68	0	0			0	0		
		16639	46538779	9.43	3.77	0.68	0	0			0	0		
	23352		385552619	9.57	3.91	0.68	0	0	34 ± 1	1	0	0		

Table 1 *continued*

Table 1 *(continued)*

Name	HD	HIP	TIC	G	M_G	$G_{BP} - G_{RP}$	Esc.	SB	$v \sin i$		δ Sct	Am	f_1	a_1
									$\mathrm{km\,s^{-1}}$	src			$\mathrm{d^{-1}}$	ppt
(1)	(2)	(3)	(4)	(5)	(6)	(7)	(8)	(9)	(10)	(11)	(12)	(13)	(14)	(15)
	23158		67768242	9.43	3.77	0.69	0	1	40 ± 1	1	0	0		
	24463		348769726	9.60	3.94	0.70	0	0			0	0		

REFERENCES

Abt, H. A. 1967, in Magnetic and Related Stars, ed. R. C. Cameron (MOno Book Co 1967 1, Baltimore), 173–+

Abt, H. A., & Levato, H. 1978, PASP, 90, 201, doi: 10.1086/130308

Aerts, C., Christensen-Dalsgaard, J., & Kurtz, D. W. 2010, Asteroseismology (Springer)

Andrae, R., Fouesneau, M., Creevey, O., et al. 2018, A&A, 616, A8, doi: 10.1051/0004-6361/201732516

Antoci, V., Cunha, M. S., Bowman, D. M., et al. 2019, MNRAS, 490, 4040, doi: 10.1093/mnras/stz2787

Astropy Collaboration. 2013, A&A, 558, A33, doi: 10.1051/0004-6361/201322068

—. 2018, AJ, 156, 123, doi: 10.3847/1538-3881/aabc4f

Baglin, A., Breger, M., Chevalier, C., et al. 1973, A&A, 23, 221

Balona, L. A., Daszyńska-Daszkiewicz, J., & Pamyatnykh, A. A. 2015, MNRAS, 452, 3073, doi: 10.1093/mnras/stv1513

Balona, L. A., & Dziembowski, W. A. 2011, MNRAS, 417, 591, doi: 10.1111/j.1365-2966.2011.19301.x

Balona, L. A., & Ozuyar, D. 2020, MNRAS, 493, 5871, doi: 10.1093/mnras/staa670

Barceló Forteza, S., Moya, A., Barrado, D., et al. 2020, A&A, 638, A59, doi: 10.1051/0004-6361/201937262

Barceló Forteza, S., Roca Cortés, T., & García, R. A. 2018, A&A, 614, A46, doi: 10.1051/0004-6361/201731803

Bastian, N., & de Mink, S. E. 2009, MNRAS, 398, L11, doi: 10.1111/j.1745-3933.2009.00696.x

Bedding, T. R., Murphy, S. J., Hey, D. R., et al. 2020, Nature, 581, 147, doi: 10.1038/s41586-020-2226-8

Belkacem, K., Goupil, M. J., Dupret, M. A., et al. 2011, A&A, 530, A142, doi: 10.1051/0004-6361/201116490

Belokurov, V., Penoyre, Z., Oh, S., et al. 2020, MNRAS, 496, 1922, doi: 10.1093/mnras/staa1522

Bovy, J. 2016, ApJ, 817, 49, doi: 10.3847/0004-637X/817/1/49

Bowman, D. M., & Kurtz, D. W. 2018, MNRAS, 476, 3169, doi: 10.1093/mnras/sty449

Brandt, T. D., & Huang, C. X. 2015, ApJ, 807, 25, doi: 10.1088/0004-637X/807/1/25

Breger, M. 1972, ApJ, 176, 367, doi: 10.1086/151641

Brown, T. M., Gilliland, R. L., Noyes, R. W., & Ramsey, L. W. 1991, ApJ, 368, 599, doi: 10.1086/169725

Castelli, F., & Kurucz, R. L. 2003, in Modelling of Stellar Atmospheres, ed. N. Piskunov, W. W. Weiss, & D. F. Gray, Vol. 210, A20. https://arxiv.org/abs/astro-ph/0405087

Chaplin, W. J., & Miglio, A. 2013, Annual Review of Astronomy and Astrophysics, 51, 353, doi: 10.1146/annurev-astro-082812-140938

Chen, J., Li, Z., Zhang, S., Deng, Y., & Zhao, W. 2022a, MNRAS, 512, 3992, doi: 10.1093/mnras/stab3589

Chen, X., Ding, X., Cheng, L., et al. 2022b, ApJS, 263, 34, doi: 10.3847/1538-4365/aca284

Creevey, O. L., Sordo, R., Pailler, F., et al. 2022, arXiv e-prints, arXiv:2206.05864. https://arxiv.org/abs/2206.05864

Curtis, J. L., Agüeros, M. A., Douglas, S. T., & Meibom, S. 2019, ApJ, 879, 49, doi: 10.3847/1538-4357/ab2393

David, T. J., Conroy, K. E., Hillenbrand, L. A., et al. 2016, AJ, 151, 112, doi: 10.3847/0004-6256/151/5/112

de Juan Ovelar, M., Gossage, S., Kamann, S., et al. 2020, MNRAS, 491, 2129, doi: 10.1093/mnras/stz3128

De Silva, G. M., Sneden, C., Paulson, D. B., et al. 2006, AJ, 131, 455, doi: 10.1086/497968

Deal, M., Goupil, M. J., Marques, J. P., Reese, D. R., & Lebreton, Y. 2020, A&A, 633, A23, doi: 10.1051/0004-6361/201936666

Debernardi, Y., Mermilliod, J.-C., Carquillat, J.-M., & Ginestet, N. 2000, A&A, 354, 881

Donati, J. F., Semel, M., Carter, B. D., Rees, D. E., & Collier Cameron, A. 1997, MNRAS, 291, 658, doi: 10.1093/mnras/291.4.658

Dupret, M.-A., Grigahcène, A., Garrido, R., Gabriel, M., & Scuflaire, R. 2005, A&A, 435, 927, doi: 10.1051/0004-6361:20041817

Dziembowski, W. 1997, in IAU Symposium, Vol. 181, Sounding Solar and Stellar Interiors, ed. J. Provost & F.-X. Schmider, 317

El-Badry, K., Rix, H.-W., & Heintz, T. M. 2021, MNRAS, 506, 2269, doi: 10.1093/mnras/stab323
Espinosa Lara, F., & Rieutord, M. 2011, A&A, 533, A43, doi: 10.1051/0004-6361/201117252
Evans, D. F. 2018, Research Notes of the American Astronomical Society, 2, 20, doi: 10.3847/2515-5172/aac173
Fox Machado, L., Pérez Hernández, F., Suárez, J. C., Michel, E., & Lebreton, Y. 2006, A&A, 446, 611, doi: 10.1051/0004-6361:20053791
Fuller, J., Hambleton, K., Shporer, A., Isaacson, H., & Thompson, S. 2017, MNRAS, 472, L25, doi: 10.1093/mnrasl/slx130
Gagné, J., Mamajek, E. E., Malo, L., et al. 2018, ApJ, 856, 23, doi: 10.3847/1538-4357/aaae09
Gaia Collaboration. 2021, A&A, 649, A1, doi: 10.1051/0004-6361/202039657
Gaia Collaboration, Babusiaux, C., et al. 2018, A&A, 616, A10, doi: 10.1051/0004-6361/201832843
Gossage, S., Conroy, C., Dotter, A., et al. 2019, ApJ, 887, 199, doi: 10.3847/1538-4357/ab5717
Goudfrooij, P., Girardi, L., & Correnti, M. 2017, ApJ, 846, 22, doi: 10.3847/1538-4357/aa7fb7
Goupil, M. J., Dupret, M. A., Samadi, R., et al. 2005, Journal of Astrophysics and Astronomy, 26, 249, doi: 10.1007/BF02702333
Gray, D. F. 2005, The Observation and Analysis of Stellar Photospheres (Cambridge Univ. Press, Cambridge)
Groenewegen, M. A. T., Decin, L., Salaris, M., & De Cat, P. 2007, A&A, 463, 579, doi: 10.1051/0004-6361:20066303
Guzik, J., Fontes, C., & Fryer, C. 2018, Atoms, 6, 31, doi: 10.3390/atoms6020031
Guzik, J. A. 2021, Frontiers in Astronomy and Space Sciences, 8, 55, doi: 10.3389/fspas.2021.653558
Guzik, J. A., Jackiewicz, J., Catanzaro, G., & Soukup, M. S. 2021, arXiv e-prints, arXiv:2107.09479. https://arxiv.org/abs/2107.09479
Handler, G. 2009, in American Institute of Physics Conference Series, Vol. 1170, Stellar Pulsation: Challenges for Theory and Observation, ed. J. A. Guzik & P. A. Bradley, 403–409, doi: 10.1063/1.3246528
Harris, C. R., Millman, K. J., van der Walt, S. J., et al. 2020, Nature, 585, 357, doi: 10.1038/s41586-020-2649-2
Hasanzadeh, A., Safari, H., & Ghasemi, H. 2021, MNRAS, 505, 1476, doi: 10.1093/mnras/stab1411
He, C., Sun, W., Li, C., et al. 2022, ApJ, 938, 42, doi: 10.3847/1538-4357/ac8b08
Hekker, S. 2020, Frontiers in Astronomy and Space Sciences, 7, 3, doi: 10.3389/fspas.2020.00003
Heyl, J., Caiazzo, I., & Richer, H. B. 2022, ApJ, 926, 132, doi: 10.3847/1538-4357/ac45fc
Houdek, G., Balmforth, N. J., Christensen-Dalsgaard, J., & Gough, D. O. 1999, A&A, 351, 582
Houdek, G., & Dupret, M.-A. 2015, Living Reviews in Solar Physics, 12, 8, doi: 10.1007/lrsp-2015-8
Hunter, J. D. 2007, Computing in Science & Engineering, 9, 90
Kamann, S., Bastian, N., Gossage, S., et al. 2020, MNRAS, 492, 2177, doi: 10.1093/mnras/stz3583
Kjeldsen, H., & Bedding, T. R. 1995, A&A, 293, 87. https://arxiv.org/abs/astro-ph/9403015
—. 2011, A&A, 529, L8, doi: 10.1051/0004-6361/201116789
Koen, C., van Rooyen, R., van Wyk, F., & Marang, F. 1999, MNRAS, 309, 1051, doi: 10.1046/j.1365-8711.1999.02928.x
Kurtz, D. W. 2022, ARA&A, 60, 31, doi: 10.1146/annurev-astro-052920-094232
Lenz, P. 2011, in New Horizons in Astronomy, 3
Li, G., Van Reeth, T., Bedding, T. R., et al. 2020, MNRAS, 491, 3586, doi: 10.1093/mnras/stz2906
Li, Z. P., Michel, E., Fox Machado, L., et al. 2002, A&A, 395, 873, doi: 10.1051/0004-6361:20021346
Lightkurve Collaboration, Cardoso, J. V. d. M., Hedges, C., et al. 2018, Lightkurve: Kepler and TESS time series analysis in Python, Astrophysics Source Code Library. http://ascl.net/1812.013
Lindegren, L., Klioner, S. A., Hernández, J., et al. 2021, A&A, 649, A2, doi: 10.1051/0004-6361/202039709
Lipatov, M., & Brandt, T. D. 2020, ApJ, 901, 100, doi: 10.3847/1538-4357/aba8f5
Maíz Apellániz, J., Pantaleoni González, M., & Barbá, R. H. 2021, A&A, 649, A13, doi: 10.1051/0004-6361/202140418

Malofeeva, A. A., Mikhnevich, V. O., Carraro, G., & Seleznev, A. F. 2023, AJ, 165, 45, doi: 10.3847/1538-3881/aca666

Marigo, P., Girardi, L., Bressan, A., et al. 2017, ApJ, 835, 77, doi: 10.3847/1538-4357/835/1/77

Martín, S., & Rodríguez, E. 2000, A&A, 358, 287

Michel, E., Dupret, M.-A., Reese, D., et al. 2017, in EPJWC, Vol. 160, EPJWC, 03001. https://arxiv.org/abs/1705.03721

Murphy, S. J., Bedding, T. R., Niemczura, E., Kurtz, D. W., & Smalley, B. 2015, MNRAS, 447, 3948, doi: 10.1093/mnras/stu2749

Murphy, S. J., Bedding, T. R., White, T. R., et al. 2022, MNRAS, 511, 5718, doi: 10.1093/mnras/stac240

Murphy, S. J., Hey, D., Van Reeth, T., & Bedding, T. R. 2019, MNRAS, 485, 2380, doi: 10.1093/mnras/stz590

Murphy, S. J., Joyce, M., Bedding, T. R., White, T. R., & Kama, M. 2021, MNRAS, 502, 1633, doi: 10.1093/mnras/stab144

Murphy, S. J., Paunzen, E., Bedding, T. R., Walczak, P., & Huber, D. 2020, MNRAS, 495, 1888, doi: 10.1093/mnras/staa1271

North, P., Ginestet, N., Carquillat, J.-M., Carrier, F., & Udry, S. 1998, Contributions of the Astronomical Observatory Skalnate Pleso, 27, 179

Pamyatnykh, A. A. 2000, in Astronomical Society of the Pacific Conference Series, Vol. 210, Delta Scuti and Related Stars, ed. M. Breger & M. Montgomery, 215

Pecaut, M. J., & Mamajek, E. E. 2013, ApJS, 208, 9, doi: 10.1088/0067-0049/208/1/9

Pérez Hernández, F., Claret, A., Hernández, M. M., & Michel, E. 1999, A&A, 346, 586

Rebull, L. M., Stauffer, J. R., Bouvier, J., et al. 2016, AJ, 152, 114, doi: 10.3847/0004-6256/152/5/114

Renson, P., & Manfroid, J. 2009, A&A, 498, 961, doi: 10.1051/0004-6361/200810788

Ricker, G. R., Winn, J. N., Vanderspek, R., et al. 2015, J. Astron. Telescopes, Instruments, and Systems, 1, 014003, doi: 10.1117/1.JATIS.1.1.014003

Riello, M., De Angeli, F., Evans, D. W., et al. 2021, A&A, 649, A3, doi: 10.1051/0004-6361/202039587

Royer, F., Zorec, J., & Gómez, A. E. 2007, A&A, 463, 671, doi: 10.1051/0004-6361:20065224

Rybizki, J., Green, G. M., Rix, H.-W., et al. 2022, MNRAS, 510, 2597, doi: 10.1093/mnras/stab3588

Sestito, P., Randich, S., & Bragaglia, A. 2007, A&A, 465, 185, doi: 10.1051/0004-6361:20066643

Southworth, J., Maxted, P. F. L., & Smalley, B. 2005, A&A, 429, 645, doi: 10.1051/0004-6361:20041867

Stateva, I., Iliev, I. K., & Budaj, J. 2012, MNRAS, 420, 1207, doi: 10.1111/j.1365-2966.2011.20108.x

Sun, W., de Grijs, R., Deng, L., & Albrow, M. D. 2019, ApJ, 876, 113, doi: 10.3847/1538-4357/ab16e4

Torres, G. 2020, ApJ, 901, 91, doi: 10.3847/1538-4357/abb136

Torres, G., Latham, D. W., & Quinn, S. N. 2021, ApJ, 921, 117, doi: 10.3847/1538-4357/ac1585

Virtanen, P., Gommers, R., Oliphant, T. E., et al. 2020, Nature Methods, 17, 261, doi: 10.1038/s41592-019-0686-2

Wang, C., Hastings, B., Schootemeijer, A., et al. 2022, arXiv e-prints, arXiv:2211.15794, doi: 10.48550/arXiv.2211.15794

Xiong, D.-r. 2021, Frontiers in Astronomy and Space Sciences, 7, 96, doi: 10.3389/fspas.2020.438870

Xiong, D. R., Deng, L., Zhang, C., & Wang, K. 2016, MNRAS, 457, 3163, doi: 10.1093/mnras/stw047

Yang, W., Bi, S., Meng, X., & Liu, Z. 2013, ApJ, 776, 112, doi: 10.1088/0004-637X/776/2/112

Zhou, G., Rodriguez, J. E., Vanderburg, A., et al. 2018, AJ, 156, 93, doi: 10.3847/1538-3881/aad085

Zorec, J., & Royer, F. 2012, A&A, 537, A120, doi: 10.1051/0004-6361/201117691